1 Preparation, Structure, and Application of Carbon Nanotubes/ Bamboo Charcoal Composite

Jiangtao Zhu[1], *Juncai Jia*[2] *and Sie Chin Tjong*[3]

[1]School for Engineering of Matter, Transport and Energy, Arizona State University, Tempe, AZ, [2]Department of Chemistry, The Chinese University of Hong Kong, Shatin, Hong Kong, China, [3]Department of Physics and Materials Science, City University of Hong Kong, Tat Chee Avenue, Kowloon, Hong Kong, China

1.1 Introduction

Naturally grown plants, such as wood and bamboo, have unique and sophisticated structures after evolution by mother nature for ages. Functional materials can be fabricated by mimicking the hierarchically build structural morphologies of renewable bioresource materials. Bamboo plants are indigenous to East Asia but are now planted in worldwide subtropical regions. The total area of bamboo forest is about 22 million ha (1 ha is 10,000 m^2), accounting for about 1.0% of the total global area of forest [1]. Although the total forest areas in many countries decrease drastically in recent years, but the bamboo vegetation increases at a rate of 3% annually. There are about 1200 types of bamboo globally. As bamboo does not need fertilizers, or pesticides, bamboo products are considered as inexpensive and eco-friendly materials. Once the bamboo is carbonized or pyrolyzed, bamboo charcoal with profuse porosity is produced. The bamboo charcoal has attracted intense attention in the past few years due to their attractive properties, including absorption, catalyst support, medical electrode, and agricultural function [2–16].

Carbon nanotubes (CNTs) exhibit excellent mechanical, thermal, and electrical properties having many functional applications [17–19]. CNTs are synthesized in large quantities by means of chemical vapor deposition (CVD) of hydrocarbon gases using transition metal or rare earth metal catalysts [18]. However, those heavy metals are toxic and pose serious problems to human health and the environment. In addition, loose CNTs are unsuitable for some applications, such as gas phase catalysis and liquid phase absorption [20]. In this regard, the successful synthesis of CNTs from bamboo charcoals is considered of technological importance. This is because bamboo charcoals containing many minerals can serve as effective

Nanocrystalline Materials. DOI: http://dx.doi.org/10.1016/B978-0-12-407796-6.00001-4

catalysts for the nucleation and growth of nanotubes. Accordingly, CNTs can be grown on a charcoal supporting material with eco-friendly characteristic.

In this chapter, the morphology, structure, and composition of the bamboo charcoal are first addressed. The processes for growing CNTs on the bamboo charcoal surfaces via CVD and arc-discharge techniques are reviewed. The role of extra catalyst added to the bamboo charcoal on the growth of CNTs at low temperatures is also discussed. Furthermore, bamboo charcoal is an excellent biomass adsorbent that has strong adsorption ability for organic pollutants and heavy metal ions. The applications of CNT/bamboo charcoal for water purification and hydrogen storage are also presented.

1.2 Bamboo Charcoal

1.2.1 Morphology, Phase, and Compositions of Bamboo Charcoal

The bamboo charcoal is usually obtained by pyrolysis bamboo in an inert atmosphere at temperatures above 700°C. The process is also termed as the carbonization in the preparation of activated carbon. During carbonization, biological bamboo releases contained water and organic gases followed by the reconstruction of carbon structure. Figure 1.1 shows typical thermogravimetry analysis (TGA) of several bamboos in a nitrogen atmosphere from room temperature to 900°C. The first mass loss at temperatures below 100°C is related to water vaporization. At 80−250°C, the mass loss of the bamboo remains stable. Then the mass drops drastically at 250−400°C due to the fast thermal decomposition of cellulose, lignin, and semicellulose. Large CO_2 and CO are released at this stage. Above 400−900°C, the mass decreases slowly. This final stage is mainly associated with the carbonization during which the aromatic rings rearrange into charcoal [21]. Four types of bamboos as shown in Figure 1.1 are used for the TGA, i.e., *Phyllostachys edulis*, *Dendrocalamus*, *Dendrocalamus brandisii*, and *Bambusa inteimedia*. Clearly, the most popular *P. edulis* has a slight different thermal property compared with other types of bamboos. Even *P. edulis* from different locations in China displays different behaviors. The *B. inteimedia* has a highest residue after the TGA process.

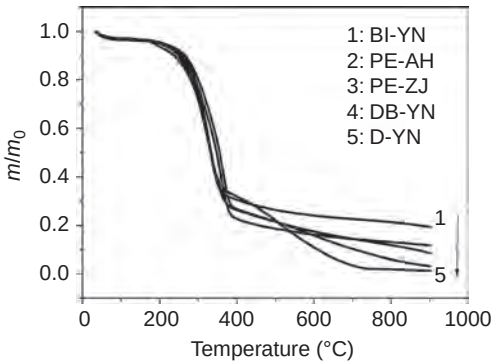

Figure 1.1 TGA of five types of bamboo: (1) BI-YN, *Bambusa*; (2) PE-AH, *Phyllostachys*; (3) PE-ZJ, *P. edulis*; (4) DB-YN, *D. brandisii*; and (5) D-YN, *Dendrocalamus*. YN, AH, and ZJ refer to Yunnan, Anhui, and Zhejiang provinces (China) where the bamboos obtained.

Generally, there is a significant volume shrinkage during the pyrolysis, however, the tubular structure of bamboo is still retained. Scanning electron microscopy (SEM) cross-sectional and lateral views show the porous feature of the bamboo charcoal carbonized at 1000°C [22] (Figure 1.2). The bamboo charcoal still retains porous nature of original bamboo. Mineral aggregates are found on the walls of vessel lumen. Jiang et al. [23] studied the shrinkage of the bamboo at different carbonization temperatures. The scaffolding of the bamboo charcoal remained the same as original bamboo, however, the microstructure of the bamboo was slightly changed during the shrinkage. The shrinkage ratios of the bamboo were about 21, 38, and 40% at 500, 750, and 1000°C, respectively. Jiang et al. also found that the wall of the parenchyma, the basic unit inside the bamboo, became rough. The outer surface of the bamboo became smooth and the whole bamboo charcoal became hard. Very recently, Zhu et al. studied the morphologies of bamboo charcoal treated at temperatures up to 1500°C. The morphologies of bamboo charcoal carbonined at 1000−1500°C retain porous feature of fresh bamboo [24]. Moreover, the bamboo charcoal exhibits a wide range of pore distribution from <1 nm to 1 μm based on the mercury porosimetry measurements (Figure 1.3). The charcoal has several dominant pore sizes (at 30, 200, 2000, and 20,000 nm), confirming hierarchical pore feature of the bamboo charcoal. The total volume of the mercury absorbed by the bamboo charcoal is about 1.7 mL/g.

The bamboo charcoal usually contains mainly carbon with a small amount of impurities. The X-ray diffraction (XRD) patterns of several bamboo charcoals prepared at

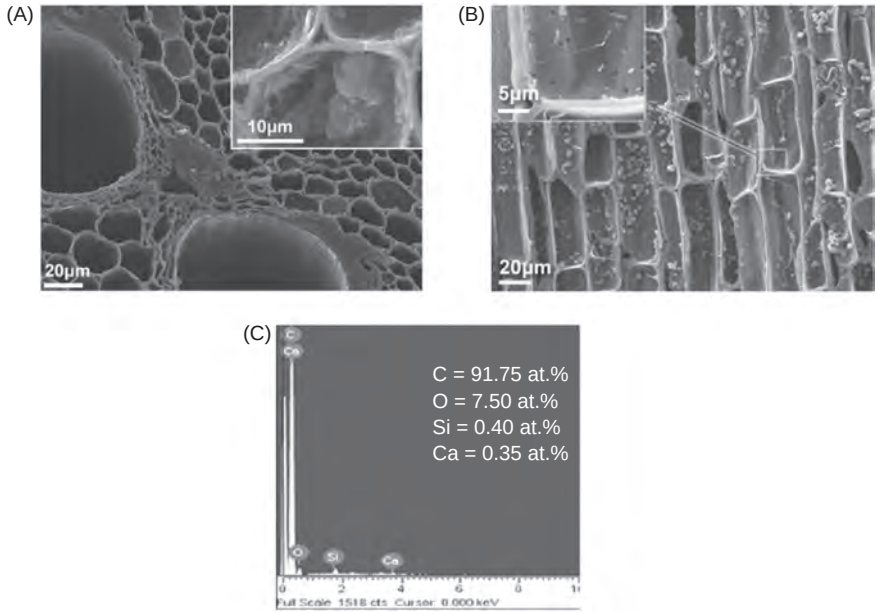

Figure 1.2 SEM images showing the (A) cross-sectional and (B) lateral views of raw bamboo biotemplate after pyrolysis and (C) corresponding EDS spectrum.
Source: Reprinted from Ref. [22] with permission of Wiley.

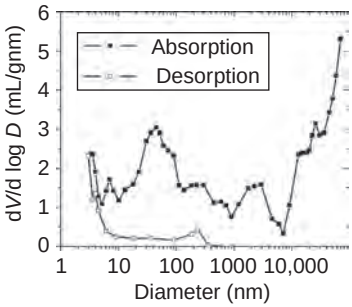

Figure 1.3 The pore structure of bamboo charcoal (*P. edulis*) revealed by absorption/desorption of mercury porosimetry.

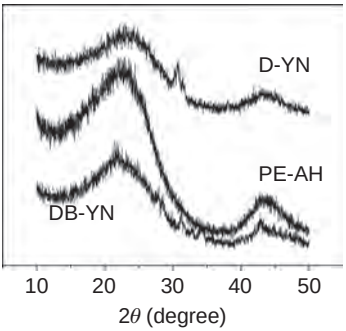

Figure 1.4 XRD patterns of D-YN, *Dendrocalamus*; PE-AH, *P. edulis*; and DB-YN, *D. brandisiss*. YN and AH refer to Province of Yunnan and Anhui (China), respectively, where the bamboos obtained.

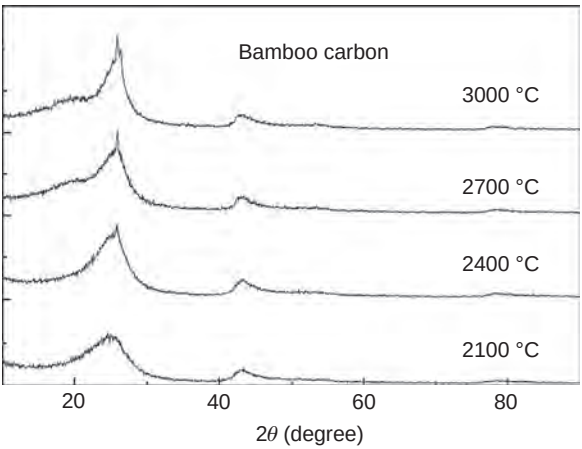

Figure 1.5 The XRD profiles of bamboo charcoal after heat treatment at different temperatures.
Source: Reprinted from Ref. [25] with permission of Springer.

800°C are shown in Figure 1.4. There are only two broad peaks located at 22 and 43°, corresponding to C_{0002} and C_{0004} reflections of carbon, respectively. Those broad peaks confirm they are mainly amorphous carbon. Chen et al. [25] (Figure 1.5) studied graphitization behavior of bamboo charcoal after carbonization up to 3000°C using XRD. The d_{0002} spacing of the bamboo charcoal decreased while the apparent graphite crystallite size L_c (0002) increased with the increase of graphitization temperatures. However, even after heat treatment at 3000°C, the d_{0002} and L_c (0002) values were only about

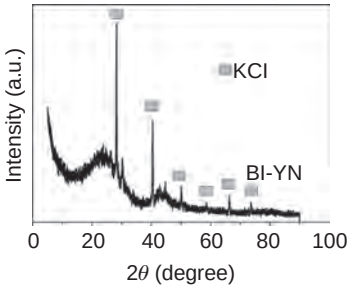

Figure 1.6 XRD patterns of BI-YN, *B. inteimedia*. YN is Yunnan province where the bamboo comes from.

0.341 and 9 nm, respectively. The bamboo charcoal is typical nongraphitizable carbon or hard carbon.

The types and amount of minerals or impurities of the bamboo charcoal depend on geological vegetation source and heat treatment history. The amount of the impurities is usually <10 wt%. X-ray energy dispersive spectroscopy (EDS) is widely recognized to be a fast and convenient route to detect the impurities. Quantitative analysis of the impurities in charcoal with higher accuracy can be determined from atomic emission spectroscopy [24]. As shown in Figure 1.2, Ca, Si, and O are found in the aggregate adhered on the pore surface of the bamboo charcoal. Jiang et al. [23] demonstrated that the bamboos (*P. edulis*) from Fujian province (China) contain many mineral elements, such as Si, N, P, K, Mg, Al in addition to C, O, H. Zhu et al. [24] identified the elements found in several types of bamboos. Bamboo (*P. edulis*) from Zhejiang province contains K, Cl, Fe, etc. Bamboo (*P. edulis*) from Anhui province contains K, Cl, Fe, Si, P, etc. Bamboo (*Dendrocalamus*) from Yunnan province contains K, Ca, Ti, Fe, Cr, Si, S, etc. Bamboo (*D. brandisii*) from Yunnan province contains Si, Ca, K, P, Mg, Fe, etc. Bamboo (*B. inteimedia*) from Yunan province contains K, Ti, Fe, Cr, Cl, Si, S, etc. The amount of KCl in bamboo (*B. inteimedia*) is so large that even it can be detected in its XRD pattern (Figure 1.6). The crystalline size is about 50 nm. The KCl should come from the soil for growing bamboos. The high amount of KCl could be one reason that its residues in TGA are higher than other types of bamboo charcoals (Figure 1.1).

1.2.2 Phases of the Minerals Inside Bamboo Charcoal

It is necessary to understand the distributions of minerals inside bamboo charcoals for designing novel bioresource materials for practical applications. Jiang et al. [23] reported that the minerals are preferrably accumulated at the outer surface of the bamboo. Zhu et al. [24] studied the evolution of minerals with carbonization temperatures. The uneven distribution of the minerals is observed for the bamboo charcoal treated at 1000°C as evidenced by EDS. Some minerals, such as K, P, Mg, S, and Ca, tend to form agglomerates. Figure 1.7 shows SEM images of bamboo charcoals pyrolyzed at high temperatures of 1200−1500°C. From the surface of charcoal pyrolyzed at 1200°C (Figure 1.7A), Mg_2SiO_4 faceted crystals of submicrometer sizes can be readily seen in the micrograph. Only spheres are found on the charcoal treated at 1300°C (Figure 1.7B) and 1400°C (Figure 1.7C). The EDS

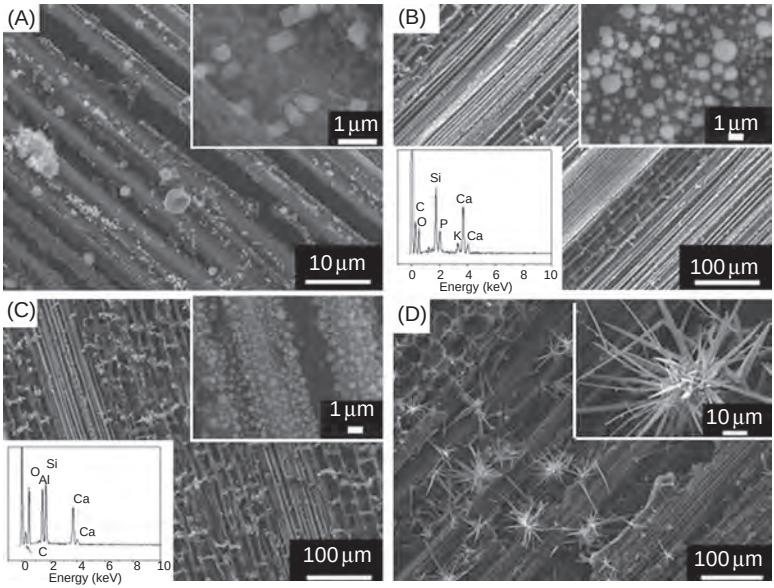

Figure 1.7 SEM images of bamboo specimens pyrolyzed at (A) 1200, (B) 1300, (C) 1400, and (D) 1500°C. Magnified images are shown in insets (top right). The bottom left insets in (B) and (C) are EDS spectra.
Source: Reprinted from Ref. [24] with permission of Elsevier.

results (insets) reveal that the spheres consist mainly of Ca, Si, and O. Trace amounts of K and P are also found inside the spheres of the charcoal treated at 1300°C. Al is detected for samples treated at 1400°C. By increasing temperature to 1500°C, SiC whiskers with lengths of about tens of micrometers are formed on the charcoal. It is interesting to note that these structures do not contain Fe.

The phases of minerals of the bamboo charcoal treated at 1000−1500°C were identified by XRD (Figure 1.8). The samples were first calcined in air at 550°C to partially remove carbon inside the charcoal. Only calcined residuals were analyzed. The residuals in the charcoal pyrolyzed at 1000°C match well with crystalline K_2SO_4 (PDF 05-0613). For the residuals of charcoals pyrolyzed at 1200°C (Figure 1.8B), three phases based on $MgSiO_3$ (PDF 88-1926), $CaSO_4$ (PDF 37-1496), and K_2SO_4 can be identified. MgO (PDF 78-0430) with low peak intensity is also detected. $MgSiO_3$ results from the decomposition of Mg_2SiO_4 during calcination at 550°C. By increasing temperature to 1300°C, only K_2SO_4 and $CaSO_4$ are detected in the residuals (Figure 1.8C). At 1400°C (Figure 1.8D), other crystalline phases such as SiC (PDF 89-1977), SiO_2 (PDF 88-2487), and CaO (PDF 77-2376) are found, while peaks due to K_2SO_4 and $CaSO_4$ become very weak. The CaO phase generates from the decomposition of $CaSO_4$. Crystalline SiO_2 is resulted from the melting and solidification of amorphous SiO_2 inside the charcoal. Crystalline SiC yields from carbothermal reduction of amorphous silica or crystalline SiO_2 phase during high-temperature pyrolysis. The above results demonstrate that the mineral phase formation in bamboo charcoals depends greatly on the heat treatment temperatures.

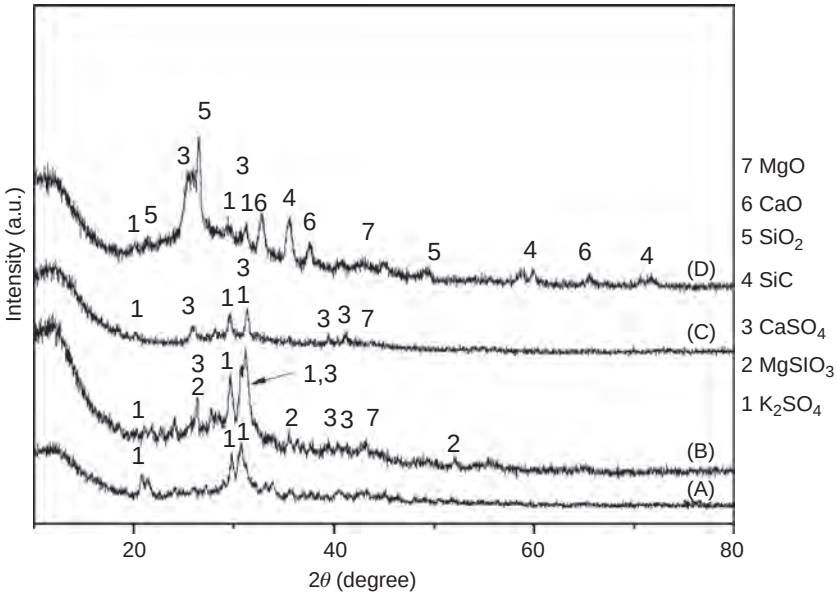

Figure 1.8 XRD spectra of the residuals of bamboo charcoals pyrolyzed at (A) 1000, (B) 1200, (C) 1300, and (D) 1400°C. (1) K_2SO_4, (2) $MgSiO_3$, (3) $CaSO_4$, (4) SiC, (5) SiO_2, (6) CaO, and (7) MgO.
Source: Reprinted from Ref. [24] with permission of Elsevier.

1.3 Functional Materials Derived from Charcoal

There is very scarce information in the literature reporting the structure of minerals inside the bamboo charcoal treated above 1500°C. Saito and Arima [26] reported the formation of cone-shaped graphitic whiskers formed inside the wood charcoal cell heat treated above 2000°C (Figure 1.9). High-resolution transmission election microscopy (HRTEM) was used to analyze the structure of synthesized graphitic whiskers. The whiskers are composed of conical stacked hexagonal carbon layers with a cone apex angle of 136°. This angle probably assisted successive helical growth of the whiskers. The growth mechanism of these whiskers was proposed. Pyrolyzed gas from the walls of the wood cells was initially released and localized mainly at the wood cell cavities. Once the gas concentration reached a supersaturation level, the whisker grew then followed the vapor−solid mode.

As discussed above, the main ingredient of the bamboo charcoal is carbon. This kind of biocarbon with special structure attracts considerable attention for preparing biomorphic materials. For example, Cheung et al. [22] converted bamboo into biomorphic composites having high purity cristobalite SiO_2 and β-SiC nanowires by sintering bamboo charcoal infiltrated with tetraethyl orthosilicate (TEOS) at 1200 and 1400°C, respectively. The fabrication process was very simple without adding

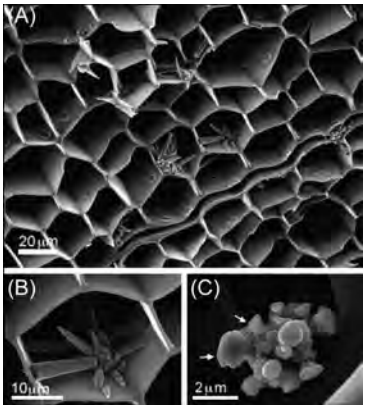

Figure 1.9 (A) SEM photographs of *Cryptomeria japonica* heat treated at 2500°C without SiC addition. (B) Magnified image of carbon deposits grown inside a wood cell. (C) Magnified image of nongrowth, nucleated substrate-like carbon. The arrows denote the cone-shaped head of nongrowth carbon clearly seen at an apex angle of 136°.
Source: Reprinted from Ref. [26] with permission of Elsevier.

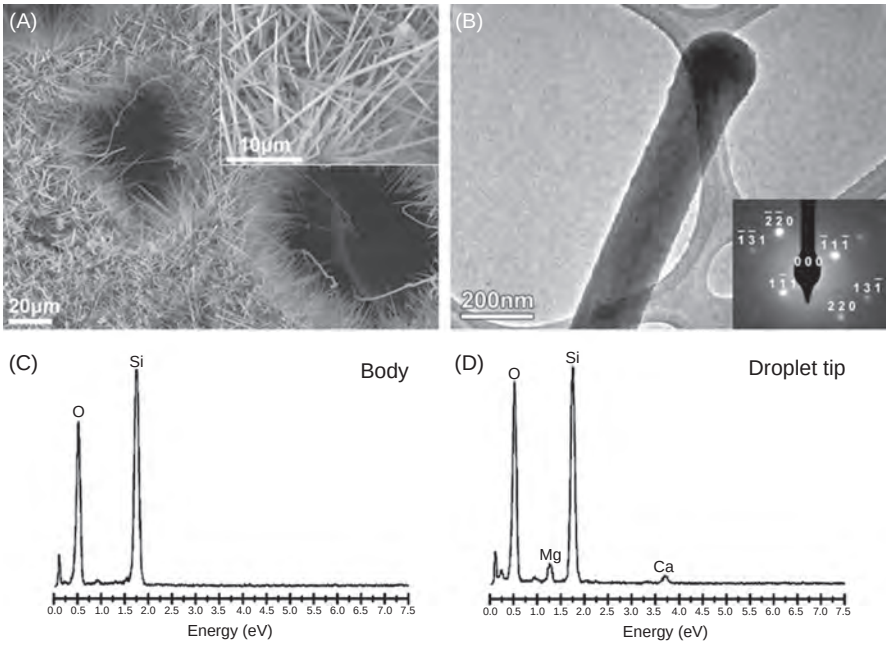

Figure 1.10 (A) SEM image of the bamboo charcoal infiltrated with TEOS sintered at 1200°C for 10 h. (B) TEM image of the top portion of a nanowire extracted from the sample shown in (A). (C and D) The TEM-EDS spectra taken at the body and droplet tip of silica nanowire shown in (B), respectively.
Source: Reprinted from Ref. [22] with permission of Wiley.

any catalysts. This is because the minerals inside bamboo charcoal can act as the catalysts. In the case of SiO_2, after sintering at 1200°C for 10 h, a thin white layer was found on the surface of the biotemplate. Figure 1.10 shows the formation of dense SiO_2 nanowires on the walls of tubular structure. EDS spectrum indicates

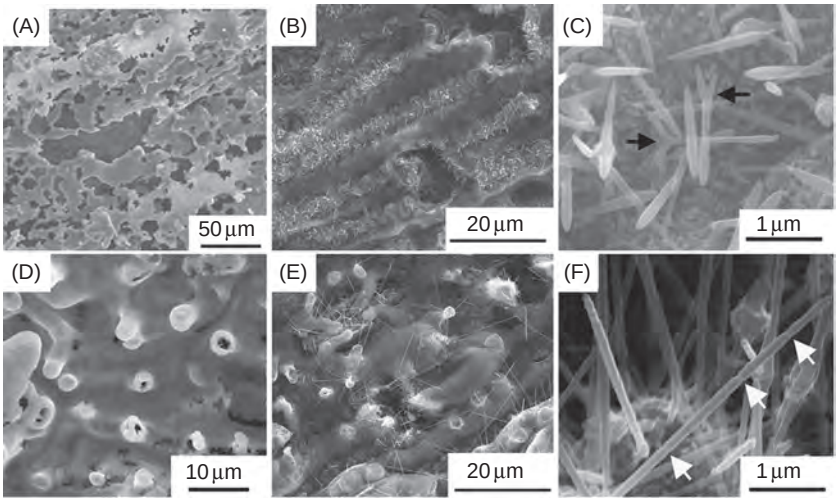

Figure 1.11 SEM images of a TEOS infiltrated bamboo leaf at 1200°C for 1 h: (A) top and (D) bottom surfaces. SEM images of a TEOS infiltrated leaf at 1300°C for 3 h: (B) the view of top surface, (C) nanowires collected from top surface, (E) the view of bottom surface, and (F) the nanowires collected from bottom surface.
Source: Reprinted from Ref. [28] with permission of Elsevier.

that the body of the nanowires contains Si and O, while its tip has <10 at.% impurities, including Mg and Ca. SiC nanowires can also be fabricated on the surface of the bamboo charcoal by a similar process at 1400°C. Zhu et al. [27] converted entire bamboo charcoal monolith into biomorphic SiC recently. Due to the complicated structure of various textures inside the bamboo, biomorphic SiC displayed different microstructures at different locations of the textures of original bamboo. Near the outer surface and large vessels of the bamboo charcoal, β-SiC nanowires were observed. In the inner part of the bamboo charcoal, such as parenchyma, sieve tube, and fibers, SiC particle aggregates that provide a high surface area for a potential support were observed.

Our recent study also reported that 6H-SiC nanowires can be synthesized from the charcoal derived from bamboo leaves [28]. Apparently, different morphologies and structures of the leaf surfaces can affect the yield and the structure of the SiC nanowires drastically. The yield of SiC grown on the top surface of the bamboo leaf is higher and with a branched structure. The SiC on the bottom surface displays a bamboo-like structure (Figure 1.11).

1.4 Synthesis of CNTs/Bamboo Charcoal

CNTs exhibit excellent mechanical, thermal, and electrical properties. In addition, CNTs also exhibit high absorbent properties. CNTs can effectively remove

different metal ions, such as cadmium, copper, lead, zinc, and nickel. However, a support is needed to immobilize CNTs due to their tiny size dimensions. Bamboo charcoal is a good support due to its low-cost, novel hierarchical structure, and high absorption ability. Due to the porous nature of bamboo charcoal, it is quite straightforward to grow CNTs on the bamboo charcoal by *in situ* synthesis method.

1.4.1 Low-Temperature CVD Method Assisted by Extra Catalyst

To grow CNTs on bamboo charcoal at low temperatures, it is necessary to load catalyst onto the charcoal initially, followed by the CVD with carbon precursor. Zhang et al. [29] impregnated bamboo charcoal initially with a ferrocene solution, then admitted volatile xylene/ferrocene through H_2/Ar carrier gas at 820°C for 20−200 min. The presence of the ferrocene was very critical for the growth of CNTs. CNTs would not form on the bamboo charcoal without using ferrocene. The prepared CNTs with a multiwall structure had curved and entangled features. The specific surface area of the bamboo charcoal dropped from 7.0 to 3.2 m^2/g after CVD growth of CNTs for 20 min. Zhang et al. also studied the effect of carbonization temperature on the growth of CNTs. Low carbonization temperature was unfavorable for the growth of CNTs.

We studied the CNTs growth on the bamboo charcoal infiltrated with $Fe(NO_3)_3$ or $Ni(NO_3)_2$ by ethanol CVD method. As shown in Figure 1.12, with the catalyst precursor $Fe(NO_3)_3$, CNTs tended to grow on the cells in both the cross-sectional and lateral directions of the bamboo charcoal after CVD process at 750°C for 30 min. The CNTs exhibited a bamboo-like structure as confirmed by the HRTEM image. Few small crystals at the end of the CNTs were observed. The EDS of the

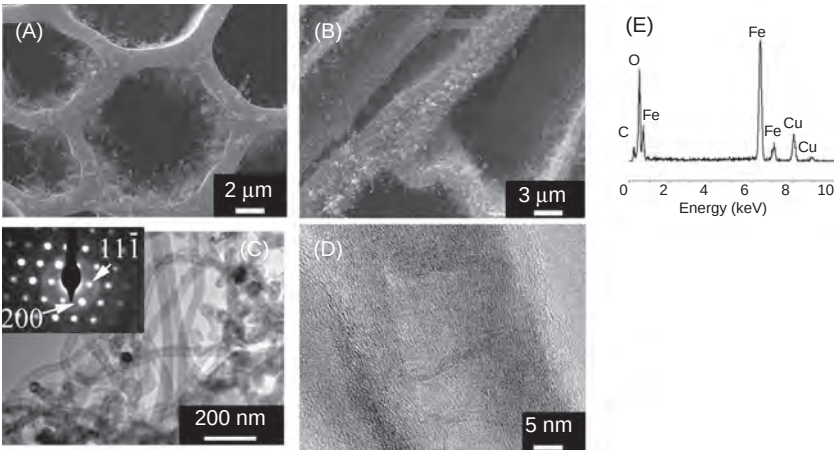

Figure 1.12 SEM images of CNTs grown on (A) cross-sectional and (B) lateral directions of bamboo charcoal by $Fe(NO_3)_3$ as catalyst precursor. (C) TEM image of CNTs with SAED from the circled crystal. (D) HRTEM of part of the CNTs showing its bamboo-like structure. (E) EDS from the circled part of (C).

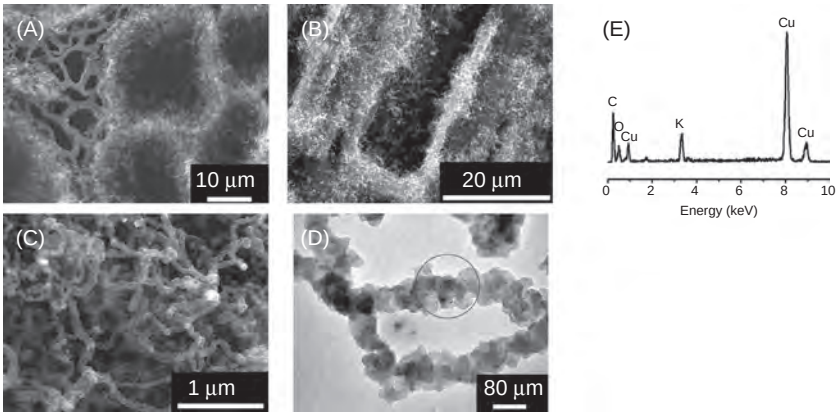

Figure 1.13 SEM images of CNTs grown on (A) cross-sectional and (B) lateral directions of the bamboo charcoal by $Ni(NO_3)_2$ as catalyst precursor. (C) SEM image of CNTs at higher magnification. (D) TEM of CNTs showing particles on their surface. (E) EDS from the circled part of (D).

crystals revealed the presence of iron and oxygen. Their selected area electron diffraction (SAED) pattern confirmed the Fe_3O_4 phase structure. When $Ni(NO_3)_2$ (Figure 1.13) was used as the catalyst precursor, CNTs of higher yield were formed on the surface of the bamboo charcoal. The CNT features were similar to those produced by Zhang et al. [29] with curved and entangled noodle appearances. The main difference was that K_2O particles from the minerals of bamboo charcoal tended to cover the surfaces of CNTs.

Recently, Chen et al. [30] reported the synthesis of carbon nanofibers (CNFs) on activated carbon produced from agricultural wastes using CVD method without adding any catalysts. They claimed that the iron inside the ash can function as the catalyst. The iron is a biologically essential element and ubiquitous in plants. In this regard, the step to upload iron catalyst onto activated carbon for the growth of CNFs is eliminated. Thus, the overall process is simplified. In the process, three activated carbons prepared from palm kernel shell (AC-P), coconut (AC-C), and wheat straw (AC-W) were first calcinated to reduce the amount of carbon but enhance the amount of impurities. Then ethylene and hydrogen were admitted during the CVD process. The iron was reduced and CNFs were grown on the surface of the three ACs (Figure 1.14). TEM image of the CNFs showed the presence of round shape of iron at their ends, revealing that iron was melted during the fiber growth (Figure 1.15). The growth mechanism of CNFs was proposed according to the tip-growing model. HRTEM examinations showed that the surface of the CNFs is rather rough. The carbon layers were not well ordered but nearly perpendicular to the axis of CNFs. Chen et al. also reported that the yield of CNFs on the ACs was not proportional to the iron content, suggesting that iron was buried in the bulk of ACs, hence not all iron took part in the CNF growth.

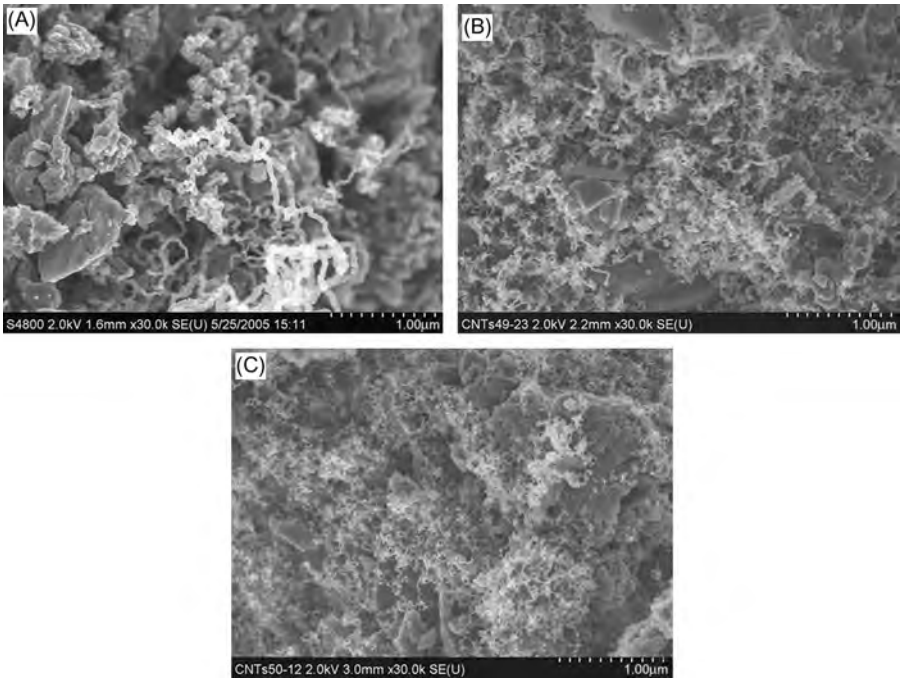

Figure 1.14 SEM images of CNFs grown on the surface of (A) AC-P, (B) AC-C, and (C) AC-W.
Source: Reprinted from Ref. [30] with permission of Elsevier.

1.4.2 Higher Temperature CVD Method Assisted by Silicate Inside Bamboo Charcoal

As discussed above, Chen et al. [30] indicated that iron element of activated carbon derived from biomass can assist the growth of CNFs at 700°C. Since iron also exists inside the bamboo, it is beneficial to use it to synthesize CNFs. To the best of our knowledge, there is no report for such synthesis of CNFs in the literature. Zhang et al. [29] mentioned that CNTs cannot grow on the bamboo charcoal without adding any iron catalyst. On the contrary, Zhu et al. [24] demonstrated that the minerals inside the bamboo charcoal can aid the growth of CNTs at temperatures of 1200−1400°C. Without adding metal catalyst, the bamboo charcoal itself was proved to be a good support and catalyst for the growth of CNTs using ethanol CVD method. CNTs were found on the surface of the bamboo charcoal between 1200 and 1400°C (Figure 1.16). Most CNTs prepared at 1300°C had round calcium silicate droplet, indicating that calcium silicate was melted during the high-temperature synthesis process. The CNTs prepared at 1400°C did not show a clear silicate droplet

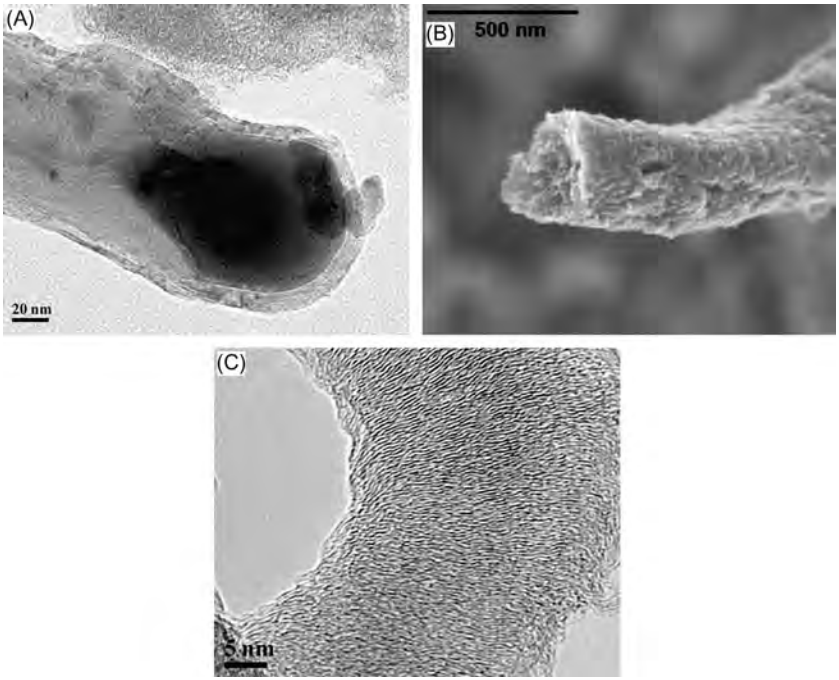

Figure 1.15 (A) TEM image of a CNF with an iron particle on its tip, (B) SEM image of a carbon nanofiber, and (C) high-resolution image of a carbon nanofiber.
Source: Reprinted from Ref. [30] with permission of Elsevier.

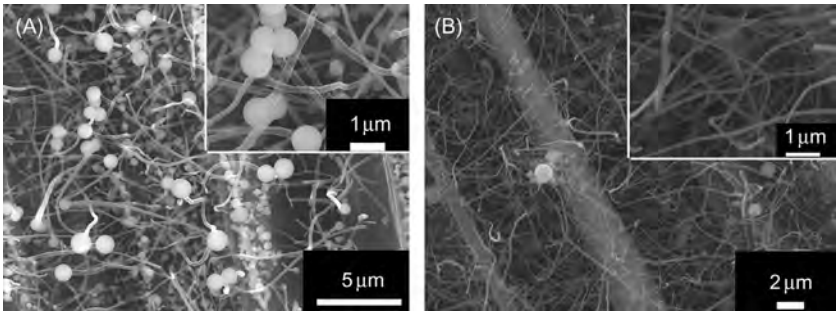

Figure 1.16 SEM images of CNTs formed on the surface of bamboo charcoal pyrolyzed at (A) 1300 and (B) 1400°C. Insets are their respective magnified images.

tip, but most CNTs were filled with silicate. TEM images were taken from the prepared CNTs, confirming hollow structure of the CNTs (Figure 1.17). The growth of CNTs was proposed to follow the vapor−liquid−solid model.

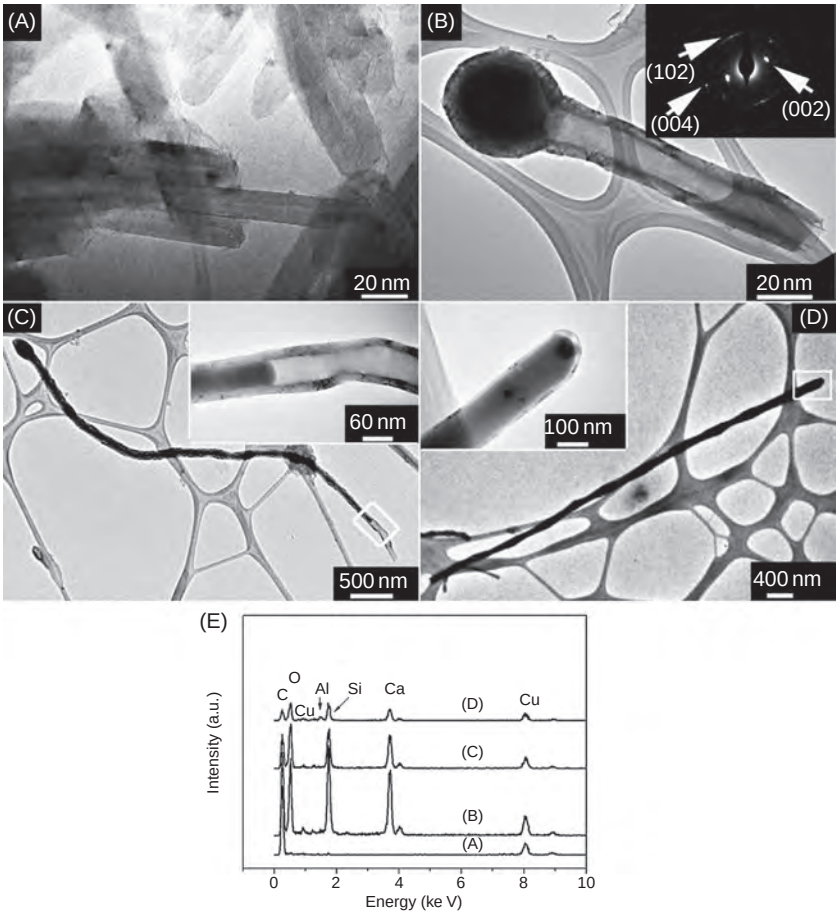

Figure 1.17 TEM images of CNTs collected from charcoal pyrolyzed at (A) 1200, (B and C) 1300, and (D) 1400°C. Inset in (B) is SAED pattern of the wall of the CNT. Insets in (C) and (D) are magnified images of rectangles. (E) EDS spectra of (A): tube in (a), (B): droplet in (b), (C): droplet in (c), and (D): filling inside the tube in (d).
Source: Reprinted from Ref. [24] with permission of Elsevier.

To exclude the role of the iron of bamboo charcoal for nucleating CNTs, Zhu et al. [31] used pure graphite as the substrate and pre-prepared calcium silicate film as a catalyst. CNT droplets filled with calcium silicate were found on the surface of the graphite, similar to the results on the bamboo charcoal. A typical CNT with a droplet end is shown in Figure 1.18. The bright and dark images confirmed that the outer shell is carbon. Electron energy-loss spectra of carbon around the droplet end and carbon in the tube body showed the existence of carbon of different bondings (Figure 1.19) [32,33]. An intense and sharp ($1s-\pi^*$) transition at 285 eV of

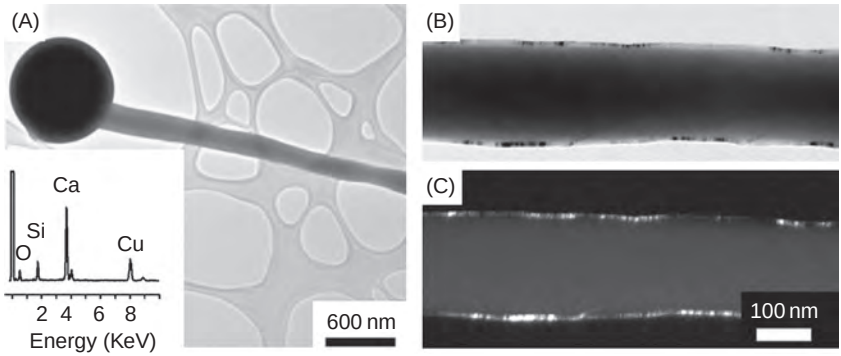

Figure 1.18 (A) TEM image of the CNTs filled with silicate, (B) bright and (C) dark field images of part of a CNT. EDS of the filling is shown as the inset.
Source: Reprinted from Ref. [31] with permission of Elsevier.

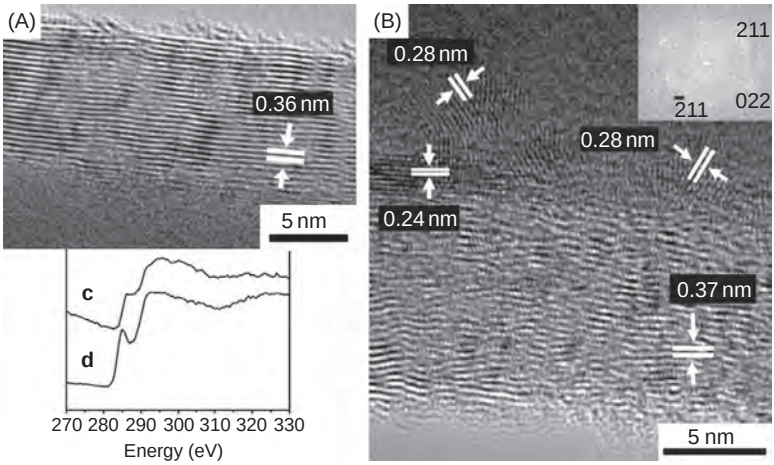

Figure 1.19 HRTEM images of CNTs (A and B). Fast Fourier transform of lattice fringe is given as the inset in (B). EELS collected from (C) the carbon around the catalyst droplet and (D) the CNT wall along the tubes.
Source: Reprinted from Ref. [31] with permission of Elsevier.

the tube wall indicated good graphene nanotexture of the CNTs. However, carbon formed around the droplet was quite amorphous. This suggested that the graphitic tube was converted from amorphous carbon around the droplet. The solid state transformation of carbon may also involve during the growth of CNTs. Since no iron is needed during the CVD process, calcium silicate apparently serves as the catalyst for the growth of CNTs. From the HRTEM observation of the wall of

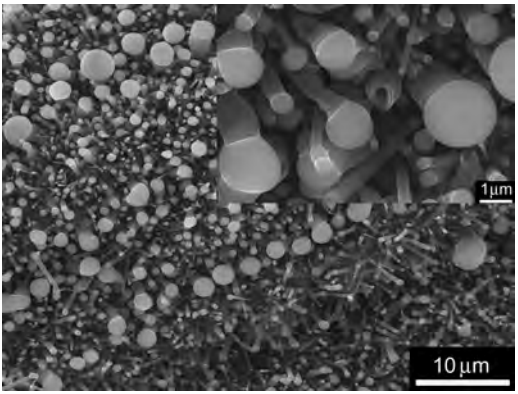

Figure 1.20 SEM image of carbon tubes grown on the surface of the bamboo charcoal by CVD method using TEOS as the source.

CNTs, the carbon layer is well crystalline, unlike the rough surface and poor crystalline CNFs prepared on the surface of activated carbon [30].

For the growth mechanism of CNTs by silicate, Zhu et al. [24] proposed that the carbon solubility in the silicate is critical for their growth. As the carbon solubility in silicate increases with the acidity, TEOS vapor acting as both carbon and silica sources is employed for increasing the acidity of silicate. During the CVD process, TEOS decomposes into silica, thereby adding more silicate into the bamboo charcoal [22]. As the same time, diethylether of TEOS also supplies carbon. Hollow CNTs with droplet ends tend to grow on the surface of the bamboo charcoal with well alignment after admitting TEOS vapor (Figure 1.20). The diameter of the carbon tubes can reach micrometer level. Small CNTs with diameter <100 nm are also found. The carbon tubes are fully filled with silicate if the amount of TEOS supplied is high enough.

1.4.3 Arc Discharge and Current Heating of Charcoal

Arc discharge is believed to be a simple and effective technique to produce high quality CNTs [18]. It is well known that crystalline CNTs can be produced by arc-discharge method using graphite as carbon source material [34,35]. In recent years, some researchers attempted to synthesize CNTs by the arc-discharge process using charcoal. For example, Fan et al. [36] successfully produced single wall carbon nanotubes (SWNTs) by direct current arc-discharge method using charcoal as the carbon source and FeS (20 wt%) as the catalyst. The diameters of synthesized SWNT bundles ranged from 10 to 40 nm (Figure 1.21). Raman spectrum showed that the ratio of integral peak intensity of G to D k was approximately 5.1, revealing that the nanotubes had a small quantity of disordered carbon or structural defect [37]. From the radial breathing mode (RBM) of SWNT, the bands at 123, 152, 167, and 187 cm^{-1} corresponded to the tube diameters of 1.2−2 nm.

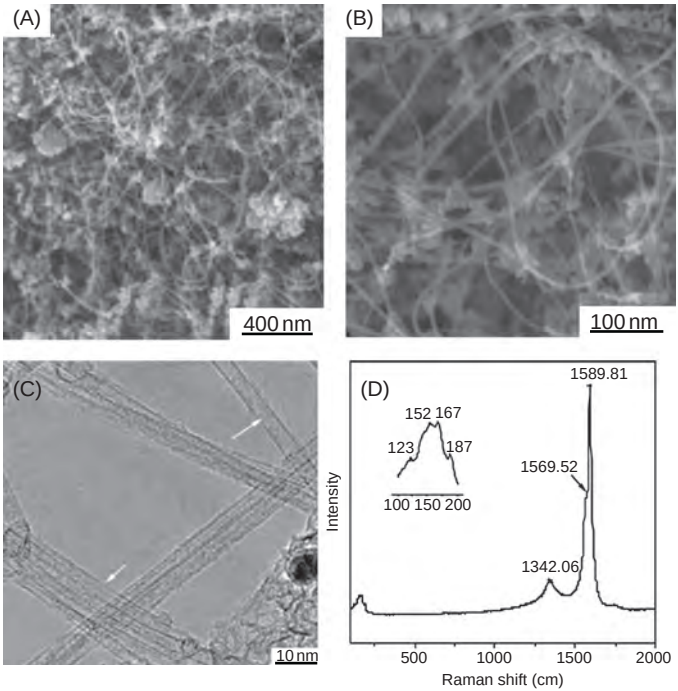

Figure 1.21 Typical SEM images of the as-prepared SWNTs obtained using FeS as catalyst by arc-discharge method: (A) low magnification image; (B) high magnification image; (C) HRTEM image; and (D) Raman spectra of the SWNTs.
Source: Reprinted from Ref. [36] with permission of Springer.

Singjai et al. [38] developed a simple and inexpensive method by heating charcoal with electrical current (CHC) to fabricate nanofibers consisting of CNTs and silicon carbide. The CHC synthesis utilizes arc-discharge facility consisting of two copper-bar electrodes, a DC power supply, and a charcoal rod. The charcoal rod was deliberately, completely, or partly broken across its middle section in order to cause poor electrical conductivity at the crack, thus inducing large current heating. After CHC, a white film was formed on the surface of charcoal rod at the cathode and at the induced crack of the rod. As shown in Figure 1.22, the fibers take the form of nanobeads. The diameter of the fibers is about 50 nm and the sizes of the beads vary from several hundred nanometers down to about 100 nm. The length of the fibers can be tens of micrometers and thus the aspect ratio is up to 1000. Singjai et al. also compared the fibers prepared by the arc discharge. The arc-discharge products have a larger diameter than the CHC fibers but with lower yield. Singjai et al. claimed that SiC was present in CHC-beaded nanofibers on the basis

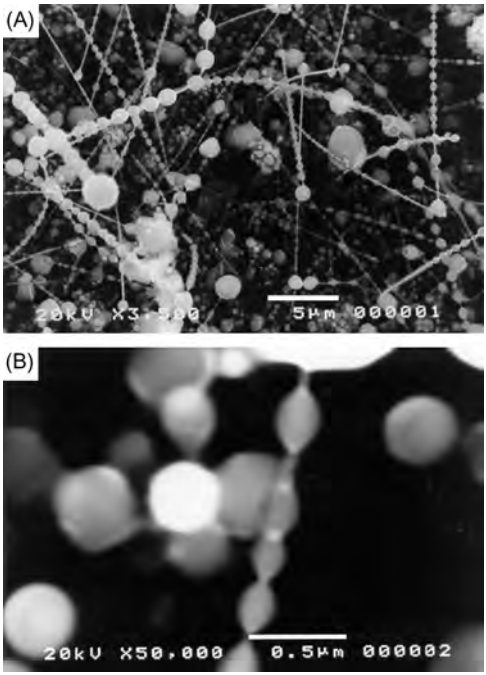

Figure 1.22 (A) SEM micrograph of nanofibers produced by the current heating of charcoal techniques in air. (B) Zoom-in image of their beads. *Source*: Reprinted from Ref. [38] with permission of Elsevier.

of XRD results. The silicon came from the charcoal. Those beaded nanofibers are excellent candidates for the reinforcements in the composte materials.

1.5 Applications of CNT/Bamboo Charcoal

CNT/bamboo charcoal composite holds multifunctional properties from both CNT and bamboo charcoal. Figure 1.23 shows the pore size distribution and nitrogen adsorption–desorption isotherms for the bamboo charcoal pyrolyzed at 1300°C with and without CNTs [24]. The average pore diameter determined from the isotherms using Barret–Joyner–Halenda (BJH) approach decreases from 7.0 to 4.5 nm after uploading of CNTs. In contrast, the adsorption volume of N_2 increases from 0.052 to 0.351 cm^3/g (inset of Figure 1.23). Moreover, the Brunauer–Emmett–Teller (BET)-specific surface area increases from 98 to 655 m^2/g.

However, Chen et al. [30] found that the BET-specific surface area, total pore and micropore volume of activated carbon, decreased drastically by growing CNFs on activated carbon. The BET value dropped from 1200 to $\sim$100 m^2/g as the CNFs filled in the pores of ACs. The size of micropores that contributed to specific surface area of activated carbon is $<$2 nm in diameter. But the diameters of synthesized CNFs are within 30–300 nm. There is little chance that CNFs can fill into micropores of ACs. Further study is needed to elucidate this problem.

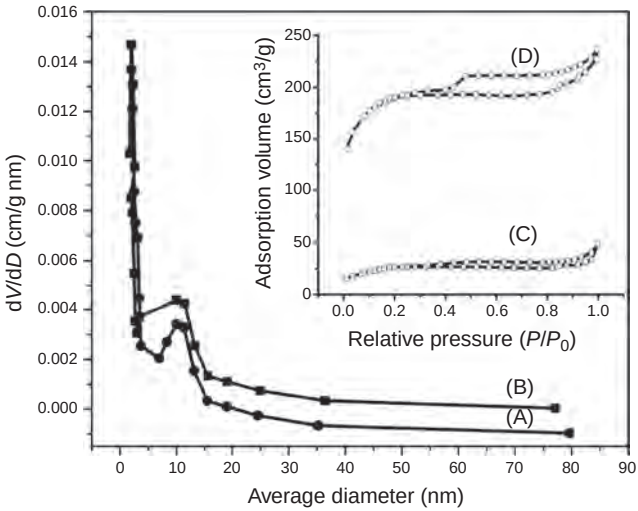

Figure 1.23 Pore size distribution of the charcoal pyrolyzed at 1300°C (A) with and (B) without the growth of CNTs. Inset: N_2 adsorption−desorption isotherms at 77 K (C) before and (D) after the growth of CNTs.
Source: Reprinted from Ref. [24] with permission of Elsevier.

1.5.1 Water Purification

The presence of excessive amounts of metal ions (copper, lead) in drinking water may accumulate in the liver of humans, thereby causing gastrointestinal problems. Activated carbon with high adsorption capability is an ideal material for removing heavy metal pollutants. Bamboo, because of its abundance and the availability, has attracted considerable attention as a carbonaceous absorbent precursor for water purification or treatment of industrial and municipal effluent. CNT/bamboo charcoal with excellent absorption properties is increasingly used in water treatment and water purification.

Zhu et al. [39] studied the absorption kinetics of bamboo-based activated carbon for phenol inside water. The absorption of phenol on the bamboo-based activated carbon generally followed the pseudo-second-order equation in which intraparticle diffusion is the rate-controlling step. The small size of activated carbon would increase the absorption rates. Zhang et al. [29] synthesized CNTs on the bamboo charcoal surface and then studied their absorption behavior for water purification. They indicated that the absorption capacity toward copper ions can be significantly improved by growing CNTs. From their results (Figure 1.24), the adsorption capacity of the CNTs/bamboo charcoal to copper ion is much higher than that of commercial activated bamboo charcoal or bamboo charcoal. An adsorption capacity of 16.34 mg/g is twice of the pristine bamboo charcoal after introducing CNTs.

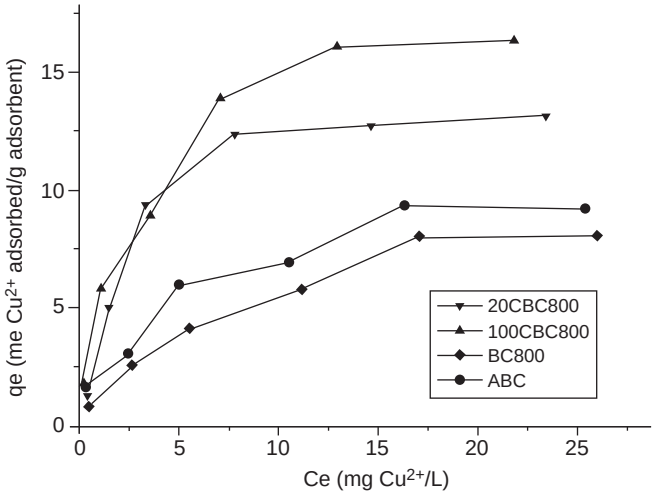

Figure 1.24 Absorption isotherm of Cu^{2+} onto four carbon samples: ABC, commercial activated bamboo charcoal; BC800, bamboo charcoal after carbonization at 800°C; 20CBC800, CNTs grown on BC800 for 20 min; 100CBC800, CNTs grown on BC800 for 100 min.
Source: Reprinted from Ref. [29] with permission of The American Chemical Society.

Huang et al. [40] studied the absorption properties of the CNT/bamboo charcoal for Pb^{2+}. As illustrated in Figure 1.25, for pristine bamboo charcoal, the amount of Pb^{2+} absorbed increased with increasing equilibrium concentration up to 24 mg/L. In contrast, the composites of the CNT/bamboo charcoal showed much larger adsorption capacity for Pb^{2+}. The amount of Pb^{2+} absorbed reached $\sim$44 mg/g for the CNT/bamboo charcoal after CVD processing for 40 min. The absorption capacity of the CNT/bamboo charcoal for lead ions is even higher than that of activated carbon and multiwall carbon nanotubes (MWCNTs). The enhanced absorption obviously benefited from the CNT additions and the increase of the acidic functional groups on the surface of the composites. The hexagonal arrays of carbon atoms in the graphite sheet of the CNT surface favor strong interactions with other molecules or atoms. Thus, CNTs grown on the bamboo charcoal surface enhance its absorption ability.

1.5.2 Hydrogen Storage

Global energy demand and weather warming have led scientists to search for alternative fuel instead of petroleum. Hydrogen is the most abundant element in the earth, has great potential as an energy source. Unlike petroleum, it can be easily generated from renewable energy sources. Thus, the safety storage of hydrogen for

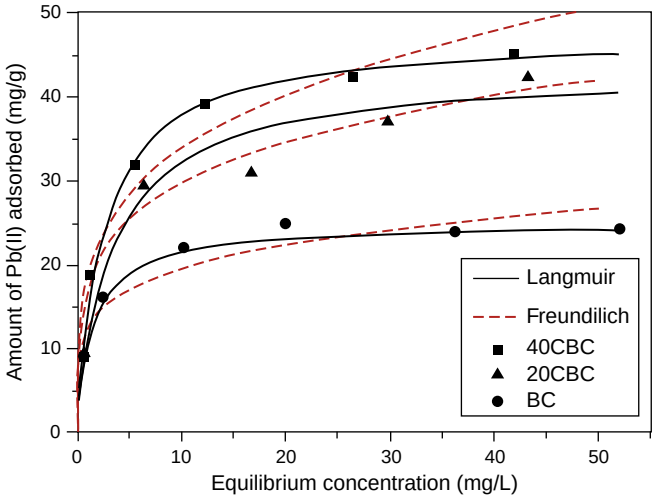

Figure 1.25 Absorption isotherms of BC and CNT/BC composites, 20CBC (20 min CVD) and 40CBC (40 min CVD), toward Pb^{2+} in aqueous solution. Curves shown in solid line are based on Langmuir equation and those in dotted line based on Freundlich equation.
Source: Reprinted from Ref. [40] with permission of Elsevier.

practical application is quite challenging. Carbon is widely known to be a promising material for hydrogen storage, especially in the form of CNTs. Porous bamboo charcoal in combination with CNTs is an ideal candidate for hydrogen storage. Miao et al. [41] studied hydrogen storage properties of SWCNTs, MWCNTs, and CNTs/bamboo charcoal (Table 1.1). The hydrogen storage of SWCNTs is the highest among those materials while the MWCNTs have the lowest value. For carbonized bamboo charcoal, its hydrogen storage is enhanced by the acid and alkali erosion, owing to the elimination of amorphous carbon and fullerence inside the materials. However, Miao also found that the hydrogen storage of bamboo charcoal is similar with or without loading CNTs.

With the aid of metal, porous materials, such as activated carbon and charcoal, are prominent hydrogen storage medium via the spillover effect. As shown in Figure 1.26, for the spillover effect, the hydrogen molecules are firstly dissociated by the doped metal clusters on the carbon surface. The resulting hydrogen atoms then diffuse away from the metal clusters and bind to the surface of the porous materials. Tsao et al. [42] studied the hydrogen spillover effect using inelastic neutron scattering. They reported that the hydrogen storage increases from 0.018% mass fraction for undoped activated carbon to 1.0% mass fraction for Pt-doped activated carbon at 66.7 kPa (500 torr). The enhancement factor is about 50. As bamboo charcoal is also a porous carbon and can be converted to activated carbon easily, it is also a promising candidate for the hydrogen storage.

Table 1.1 The Comparison of Hydrogen Storage in SWCNTs, MWCNTs, and Taiwan Bamboo Charcoal

Materials		Hydrogen Storage
Carbon nanotubes	SWCNTs	0.668 wt%
	MWCNTs (grown by arc discharge)	0.219 wt%
	MWCNTs (grown by arc discharge and purified)	0.588 wt%
Taiwan bamboo charcoal	Virgin	0.431 wt%
	Pretreatment by 70% nitric acid after 24 h	0.522 wt%
	Pretreatment by 6 M KOH after 24 h	0.569 wt%
	Bamboo charcoal with CNTs grown by arc discharge	0.462 wt%
	Bamboo charcoal with CNTs grown by MPECVD	0.520 wt%

Source: Reproduced courtesy of The Electromagnetics Academy [41].

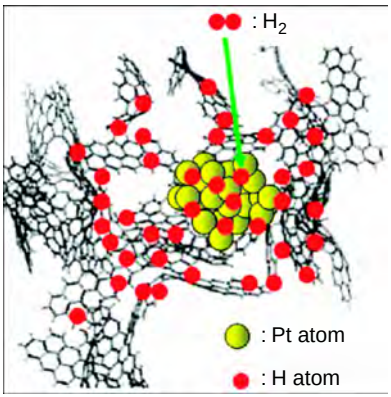

Figure 1.26 Scheme to show the hydrogen spillover on Pt cluster uploaded on activated carbon.
Source: Reprinted from Ref. [42] with permission of The American Chemical Society.

1.6 Conclusions

Novel, inexpensive, multifunctional composites based on CNT/bamboo charcoal are introduced in this chapter. Their fabrication method, structure, and application are addressed. Bamboo charcoal is an eco-friendly biocarbon obtained by pyrolyzing bamboos at high temperatures. It exhibits porous structure and contains amorphous carbon and a small amount of minerals. The types of mineral elements depend mainly on the geological regions of bamboo vegetation. The minerals inside the bamboo charcoal can transform into various phases and structures under different calcination temperatures. For example, SiC nanowhiskers are formed on the bamboo charcoal surface by heating at 1500°C. To grow CNTs on bamboo charcoal at low temperatures (700−800°C), ethanol CVD assisted by extra metal catalysts (e.g., iron, nickel) is employed. At 1200−1500°C, the minerals inside

charcoal are beneficial for the nucleation and growth of CNTs. The CNT/bamboo charcoal exhibits excellent absorption properties for removing metal ion pollutants. Finally, bamboo charcoals with or without CNTs are ideal materials for hydrogen storage.

References

[1] Zhou GM, Meng CF, Jiang PK, Xu QF. Review of carbon fixation in bamboo forests in China. Bot Rev 2011;77(3):262–70.

[2] Liao P, Yuan S, Xie W, Zhang W, Tong M, Wang K. Adsorption of nitrogen-heterocyclic compounds on bamboo charcoal: kinetics, thermodynamics, and microwave regeneration. J Colloid Interface Sci 2013;390(1):189–95.

[3] Liao P, Yuan S, Zhang W, Tong M, Wang K. Mechanistic aspects of nitrogen-heterocyclic compound adsorption on bamboo charcoal. J Colloid Interface Sci 2012;382(1):74–81.

[4] Zhang H, Zhu G, Jia X, Ding Y, Zhang M, Gao Q, et al. Removal of microcystin-LR from drinking water using a bamboo-based charcoal adsorbent modified with chitosan. J Environ Sci (China) 2011;23(12):1983–8.

[5] Wang M, Huang ZH, Liu G, Kang F. Adsorption of dimethyl sulfide from aqueous solution by a cost-effective bamboo charcoal. J Hazard Mater 2011;190 (1–3):1009–15.

[6] Wang FY, Wang H, Ma JW. Adsorption of cadmium (II) ions from aqueous solution by a new low-cost adsorbent—bamboo charcoal. J Hazard Mater 2010;177 (1–3):300–6.

[7] Mizuta K, Matsumoto T, Hatate Y, Nishihara K, Nakanishi T. Removal of nitrate-nitrogen from drinking water using bamboo powder charcoal. Bioresour Technol 2004;95(3):255–7.

[8] Chuang CS, Wang MK, Ko CH, Ou CC, Wu CH. Removal of benzene and toluene by carbonized bamboo materials modified with TiO_2. Bioresour Technol 2008;99 (5):954–8.

[9] Kosuwon W, Laupattarakasem W, Saengnipanthkul S, Mahaisavariya B, Therapongpakdee S. Charcoal bamboo as a bone substitute: an animal study. J Med Assoc Thai 1994;77(9):496–500.

[10] Venkatesan N, Yoshimitsu J, Ito Y, Shibata N, Takada K. Liquid filled nanoparticles as a drug delivery tool for protein therapeutics. Biomaterials 2005;26(34):7154–63.

[11] Hsieh MF, Wen HW, Shyu CL, Chen SH, Li WT, Wang WC, et al. Synthesis, *in vitro* macrophage response and detoxification of bamboo charcoal beads for purifying blood. J Biomed Mater Res A 2010;94(4):1133–40.

[12] Lin CC, Ni MH, Chang YC, Yeh HL, Lin FH. A cell sorter with modified bamboo charcoal for the efficient selection of specific antibody-producing hybridomas. Biomaterials 2010;31(32):8445–53.

[13] Yang S, Jia B, Liu H. Effects of the Pt loading side and cathode biofilm on the performance of a membrane-less and single-chamber microbial fuel cell. Bioresour Technol 2009;100(3):1197–202.

[14] Hua L, Chen Y, Wu W. Impacts upon soil quality and plant growth of bamboo charcoal addition to composted sludge. Environ Technol 2012;33(1–3):61–8.

[15] Xu T, Lou L, Luo L, Cao R, Duan D, Chen Y. Effect of bamboo biochar on pentachlorophenol leachability and bioavailability in agricultural soil. Sci Total Environ 2012;414:727–31.
[16] Gao H, Zhang Z, Wan X. Influences of charcoal and bamboo charcoal amendment on soil-fluoride fractions and bioaccumulation of fluoride in tea plants. Environ Geochem Health 2012;34(5):551–62.
[17] Thostenson ET, Ren ZF, Chou TW. Advances in the science and technology of carbon nanotubes and their composites: a review. Compos Sci Technol 2001;61 (13):1899–912.
[18] Tjong SC, Chen H. Nanocrystalline materials and coatings. Mater Sci Eng R 2004;45 (1–2):1–88.
[19] Zhu JT, Tjong SC, Li XQ. Spark plasma sintered hydroxyapatite/multiwalled carbon nanotube composites with preferred crystal orientation. Adv Eng Mater 2010;12 (11):1161–5.
[20] Lam CW, James JT, McCluskey R, Arepalli S, Hunter RL. A review of carbon nanotube toxicity and assessment of potential occupational and environmental health risks. Crit Rev Toxicol 2006;36(3):189–217.
[21] Zuo SL, Gao SY, Yuan XG, Xu BS. Carbonization mechanism of bamboo (*Phyllostachys*) by means of Fourier transform infrared and elemental analysis. J Forestry Res 2003;14(1):75–9.
[22] Cheung TLY, Ng DHL. Conversion of bamboo to biomorphic composites containing silica and silicon carbide nanowires. J Am Ceram Soc 2007;90(2):559–64.
[23] Jiang ZH, Zhang DS, Fei BH, Yue YD, Chen XH. Effects of carbonization temperature on the microstructure and electrical conductivity of bamboo charcoal. New Carbon Mater 2004;19(4):249–53.
[24] Zhu JT, Jia JC, Kwong FL, Ng DHL, Tjong SC. Synthesis of multiwalled carbon nanotubes from bamboo charcoal and the roles of minerals on their growth. Biomass Bioenerg 2012;36:12–9.
[25] Cheng HM, Endo H, Okabe T, Saito K, Zheng GB. Graphitization behavior of wood ceramics and bamboo ceramics as determined by X-ray diffraction. J Porous Mater 1999;6(3):233–7.
[26] Saito Y, Arima T. Features of vapor-grown cone-shaped graphitic whiskers deposited in the cavities of wood cells. Carbon 2007;45(2):248–55.
[27] Zhu JT, Kwong FL, Ng DHL. Synthesis of biomorphic SiC ceramic from bamboo charcoal. J Nanosci Nanotechnol 2009;9(2):1564–647.
[28] Zhu J, Jia J, Kwong FL, Ng DHL. Synthesis of 6 H-SiC nanowires on bamboo leaves by carbothermal method. Diamond Relat Mater 2013;33:5–11.
[29] Zhang JN, Huang ZH, Lv R, Yang QH, Kang FY. Effect of growing CNTs onto bamboo charcoals on adsorption of copper ions in aqueous solution. Langmuir 2009;25 (1):269–74.
[30] Chen XW, Timpe O, Hamid SBA, Schlogl R, Su DS. Direct synthesis of carbon nanofibers on modified biomass-derived activated carbon. Carbon 2009;47(1):340–3.
[31] Zhu JT, Jia JC, Kwong FL, Ng DHL, Crozier PA. Metal-free synthesis of carbon nanotubes filled with calcium silicate. Carbon 2012;50(7):2666–9.
[32] Egerton RF. Electron energy-loss spectroscopy in the TEM. Rep Prog Phys 2009;72 (1): 016502 (25pp.).
[33] Egerton RF. Electron energy-loss spectroscopy in the electron microscope. 3rd ed. New York: Springer; 2011.

[34] Ajayan PM, Redlich P, Ruhle M. Balance of graphite deposition and multishell carbon nanotube growth in the carbon arc discharge. J Mater Res 1997;12(1):244–52.
[35] Gamaly EG, Ebbesen TW. Mechanism of carbon nanotube formation in the arc-discharge. Phys Rev B 1995;52(3):2083–9.
[36] Fan WW, Zhao J, Lv YK, Bao WR, Liu XG. Synthesis of SWNTs from charcoal by arc-discharging. J Wuhan Univ Technol 2010;25(2):194–6.
[37] Zhu JT, Kwong FL, Lei M, Ng DHL. Synthesis of carbon coated silica nanowires. Mater Chem Phys 2010;124(1):88–91.
[38] Singjai P, Wongjamras A, Yu LD, Tunkasiri T. Production and characterization of beaded nanofibers from current heating of charcoal. Chem Phys Lett 2002;366 (1–2):51–5.
[39] Zhu JT, Huang ZH, Kang FY, Fu JH, Yue YD. Adsorption kinetics of activated bamboo charcoal for phenol. New Carbon Mater 2008;23(4):326–30.
[40] Huang ZH, Zhang FZ, Wang MX, Lv RT, Kang FY. Growth of carbon nanotubes on low-cost bamboo charcoal for Pb(II) removal from aqueous solution. Chem Eng J 2012;184:193–7.
[41] Miao HY, Chang LW, Lue JT, editors. PIERS Proceedings, Hangzhou, China, March 24–28. Cambridge, MA: The Electromagnetics Academy; 2008.
[42] Tsao CS, Liu Y, Chuang HY, Tseng HH, Chen TY, Chen CH, et al. Hydrogen spillover effect of Pt-doped activated carbon studied by inelastic neutron scattering. J Phys Chem Lett 2011;2(18):2322–5.